3 Biotech (2022) 12:60
https://doi.org/10.1007/s13205-022-03125-2

ORIGINAL ARTICLE

Isolation and acetylcholinesterase inhibitory activity of asterric acid derivatives produced by *Talaromyces aurantiacus* FL15, an endophytic fungus from *Huperzia serrata*

Yiwen Xiao[1,2] · Weizhong Liang[2] · De Liu[1] · Zhibin Zhang[1] · Jun Chang[2] · Du Zhu[1,2]

Received: 27 July 2021 / Accepted: 23 January 2022 / Published online: 5 February 2022

Abstract

Alzheimer's disease (AD) is a neurodegenerative disease and the fourth leading cause of death after cardiovascular disease, tumors, and stroke. Acetylcholinesterase (AChE) inhibitors, which are based on cholinergic damage, remain the mainstream drugs to alleviate AD-related symptoms. This study aimed to explore novel AChE inhibitors produced by the endophytic fungus FL15 from *Huperzia serrata*. The fungus was identified as *Talaromyces aurantiacus* FL15 according to its morphological characteristics and ITS, 18S rDNA, and 28S rDNA sequence analysis. Subsequently, seven natural metabolites were isolated from strain FL15, and identified as asterric acid **(1)**, methyl asterrate **(2)**, ethyl asterrate **(3)**, emodin **(4)**, physcion **(5)**, chrysophanol **(6)**, and sulochrin **(7)**. Compounds **1–3**, which possess a diphenyl ether structure, exhibited highly selective and moderate AChE inhibitory activities with IC_{50} values of 66.7, 23.3, and 20.1 μM, respectively. The molecular docking analysis showed that compounds **1–3** interacted with the active catalytic site and peripheral anionic site of AChE, and the esterification substitution groups at position 8 of asterric acid may contribute to its bioactivity. The asterric acid derivatives showed highly selective and moderate AChE inhibitory activities, probably via interaction with the peripheral anionic site and catalytic site of AChE. To the best of our knowledge, this study was the first report of the AChE inhibitory activity of asterric acid derivatives, which opens new perspectives for the design of more effective derivatives that could serve as a drug carrier for new chemotherapeutic agents to treat AD.

Keywords Endophytic fungi · *Talaromyces aurantiacus* FL15 · Asterric acid · Acetylcholinesterase inhibitors

Introduction

Alzheimer's disease (AD), which is commonly known as dementia, is a neurodegenerative disorder characterized by memory loss and other cognitive impairments (Jalili-Baleh et al. 2018; Friker et al. 2020). Reportedly, over 46 million people live with dementia worldwide, and the evaluated number is expected to increase to 131.5 million by 2050 (Prince et al. 2015). The rapid growth of AD has led many medicinal chemists to develop drug-discovery investigations in this field (Prince et al. 2015; Mohammadi-Khanaposhtani et al. 2015; Friker et al. 2020).

The etiology of AD is not well understood. Thus, different pathogenesis hypotheses regarding AD, including cholinergic, amyloid cascade, oxidative stress, and tau protein, have been proposed. Among them, the cholinergic hypothesis is widely accepted (Goedert and Spillantini 2006; Sonmez et al. 2017; Oh et al. 2019). According to this hypothesis, the most effective therapeutic approach for treating AD is the restoration of the acetylcholine (ACh) levels in the brain by inhibiting acetylcholinesterase (AChE). AChE inhibitors (AChEIs) can effectively improve neurotransmitter activity levels and duration by inhibiting the hydrolysis of ACh (Sonmez et al. 2017; Oh et al. 2019). Currently, the mainstay drugs used for the clinical management of AD remain AChEIs. Four AChEIs, namely, tacrine, donepezil, galantamine, and rivastigmine, have been approved by European and US agencies (Sonmez et al. 2017; Oh et al. 2019).

✉ Du Zhu
zhudu12@163.com

[1] Key Laboratory of Protection and Utilization of Subtropic Plant Resources of Jiangxi Province, College of Chemistry and Chemical Engineering, Jiangxi Normal University, Nanchang 330022, Jiangxi, People's Republic of China

[2] Key Lab of Bioprocess Engineering of Jiangxi Province, College of Life Sciences, Jiangxi Science and Technology Normal University, Nanchang 330013, China

Huperzine A (Hup A), a powerful and selective lycopodium alkaloid AChEI firstly isolated from Qian Ceng Ta (i.e., *Huperzia serrata*) in traditional Chinese medicine, was also approved in the 1990s in China (Fig. 1) (Ma et al. 2007). Although the existing AChEI drugs are essential for palliating AD, their clinical efficacy is limited because of their poor selectivity, low bioavailability, and adverse side effects on the peripheral nervous system and liver. Therefore, great efforts have been dedicated for investigating better and novel AChEIs from natural sources (Zaki et al. 2020).

Fungi are important organisms in the production of bioactive secondary metabolites. Currently, many of the drugs in the market that possess various activities, such as antitumor, immunosuppressant, antibiotic, hypocholesterolemic, antifungal, antiparasitic, anti-inflammatory, and enzyme-inhibiting activities, were obtained from fungal metabolism (Kingston 2011; Teles and Takahashi 2013). Endophytic fungi are microorganisms that reside in the internal tissues of living plants or animals without causing apparent disease (Gupta et al. 2019). Endophytes, an eclectic group of microbes that can chemically bridge the gap between plants and microbes, have attracted the most attention because of their relatively high metabolic versatility (Zaki et al. 2020). Thus, endophytes have been demonstrated to be a rich source of bioactive metabolites with diverse structural features, and a large number of compounds with novel structures and various bioactivities are continuously being isolated from them (Gupta et al. 2019; Zaki et al. 2020). Notably, some endophytic fungi have produced identical or similar chemical compounds to those produced by their host. For example, the widely prescribed anticancer drug paclitaxel (Taxol), one of the most amazing natural products initially isolated from the Pacific yew tree *Taxus brevifolia*, was later found in the endophytic fungus *Taxomyces andreanae* and other fungal genera (Liu et al. 2016). Hup A was also found in the endophytic fungus *Shiraia* sp. Slf14, as well as in *Cladosporium cladosporioides* LF70, *Penicillium* sp. LDL4.4, *Trichoderma harzianum* L44, and other endophytic fungi (Ellman et al. 1961; Zhang et al. 2011; Cao et al. 2021).

The endophytic fungi from *H. serrata* are a huge untapped source of natural products including AChEI. Thus far, there are only few reports on AChEI form endophytic fungi of *H. serrata* (Cao et al. 2021). In our previous screening studies, a total number of 22 endophytic fungi strains, including strain FL15, showed high AChE inhibitory activity (≥50%) (Wang et al. 2016b). In the present study, as part of an ongoing search for Hup A-producing endophytes and new natural AChEI, the secondary metabolites from the ethyl acetate extract of fungal strain FL15 were isolated, and seven natural metabolites were purified and identified. AChE inhibition

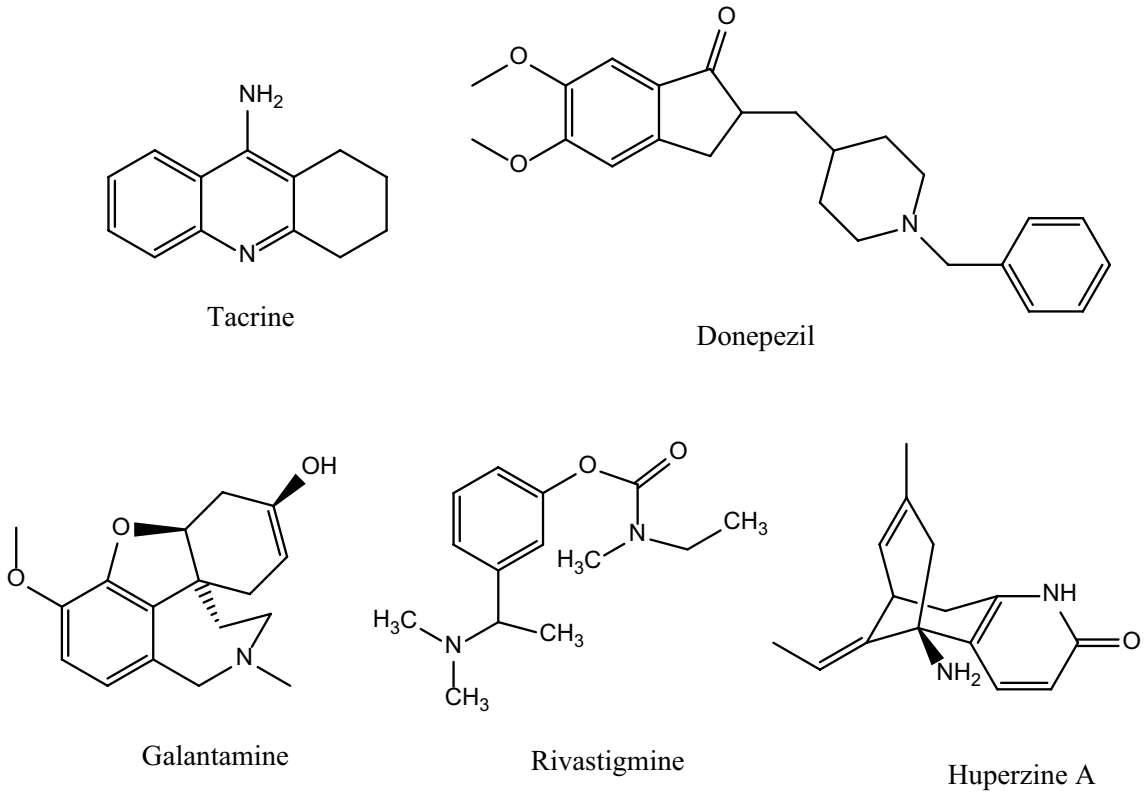

Fig. 1 Chemical structures of the main acetylcholinesterase inhibitors used in clinical management

results showed that the three asterric acid derivatives exhibited highly selective and moderate AChE inhibitory activities. Then, the molecular docking analysis was carried out to reveal the binding patterns between the three asterric acid derivatives and AChE proteins. This study not only provided new precursors of the anti-AChE drug, but also contributed to the application of endophytic fungi as compounds producers in biopharmaceutical industry.

Materials and methods

General

The strain FL15 used in this study was isolated from the leaves of *H. serrata*, which were collected from natural populations at Lushan Botanical Garden in Jiangxi Province, Central China. This strain was subsequently deposited in the China Center for Type Culture Collection (CCTCC NO: 2019832), Wuhan, China.

^{1}H and ^{13}C data were acquired on a Bruker AV400 spectrometer at 400 and 100 MHz, respectively, using $CDCl_3$, acetone-d_6, and CD_3OD as solvents. Chemical shifts were given in parts per million (δ) using tetramethylsilane (TMS) as an internal standard. *J* values were given in Hertz. Abbreviations for the ^{1}H NMR data quoted are as follows: s, singlet; d, doublet; t, triplet; q, quartet; m, multiplet; bs, broad singlet. ESI–MS data were recorded on a Waters Xevo G2 quadrupole time-of-flight/time-of-flight (QTof/Tof) mass spectrometer (Milford, Massachusetts, USA). High-performance liquid chromatography (HPLC) was performed on a Waters W2996 chromatograph equipped with a 1525 pump using a C18 column (19 × 150 mm, 5 µm; YMC Co., Ltd.).

Chemicals and enzymes

All solvents and reagents were obtained from commercial sources, unless stated otherwise. Electric eel acetylcholinesterase (AChE, Type-VI-S, EC 3.1.1.7, 425.84 U/mg, Sigma) and equine serum butyrylcholinesterase (BuChE, E.C.3.1.1.8) were purchased from Sigma (Steinheim, Germany). Acetylthiocholine iodide (AChI), butyrylthiocholine iodide (BChI), and dithiobis nitrobenzoic acid (DTNB) were purchased from Sigma-Aldrich (Taufkirchen, Germany). The solvents used for chromatography were of HPLC grade, whereas the solvents used for extraction were of American Chemical Society grade. Silica gel (200–300 mesh, Qingdao Marine Chemical Group Co., Ltd. Qingdao, China) and Sephadex LH-20 (25–100 µm; Amersham Biosciences) were used for column chromatography. Thin-layer chromatography (TLC) was performed with glass-precoated silica gel 60 plates (0.25 mm; Merck, Darmstadt, Germany). Other chemicals were from China Medicine Shanghai Chemical Reagent Co., Ltd.

Identification of the endophytic fungus FL15

The endophytic fungus FL15 was identified by morphological observation combined with the determination of the sequences of the rDNA internal transcribed spacer (ITS), 18S rDNA, and 28S rDNA (Lai et al. 2014).

A small number of mycelia were selected from the preserved brilliant medium, and the strains were inoculated into potato dextrose agar (PDA), yeast extract sucrose agar (YES), and Czapek yeast extract agar (CYA) plate medium using the point-planting method, respectively. The strains were cultured in a 28 °C constant temperature incubator for 10–20 days, of culture, and the changes in, and characteristics of, colony morphology were regularly observed: the shape, size, texture, color, edge characteristics, and other conditions of the colony were recorded (Lai et al. 2014). After sampling, the morphology of the mycelium was observed under an optical microscope (BA300, Motic, China) after alkaline methylene blue staining and a scanning electron microscope (SEM, QUANTA-200F, FEI, The Netherlands).

The strains were inoculated into a liquid medium and cultured at 28 °C and 150 rpm for 14 days. The mycelia were filtered for molecular biological identification. Genomic DNA was extracted using the improved CTAB method (Zhang et al. 1996). The ITS, 18S, and 28S sequences of the FL15 strain were amplified. The amplified sequences were detected via 1% agar electrophoresis gel, and the gel plate was stained with ethidium bromide. After detection of the bands, the PCR products were sent to Sangon Biotech (Shanghai) Co., Ltd. for sequencing, to obtain the relevant gene sequence fragments. The fragments were uploaded to the GenBank database of the National Center for Biotechnology Information (NCBI) for Basic Local Alignment Search Tool (BLAST) comparison, and the application number was obtained. Moreover, a phylogenetic analysis was performed using the MEGA 7.0.14 ClustalX software, and an evolutionary tree was constructed to determine the classification status of the strain (Vig et al. 2021).

Fermentation and extraction of mycelia

The fungal strain FL15 was cultured on slants of PDA at 28 °C for 7 days. The mycelia from the PDA plate were harvested and grown in 150 mL of PDB medium for 5 days at 28 °C and 150 rpm. Aliquots (5 mL) of this seed culture were inoculated into 500 mL Erlenmeyer flasks that contained 100 mL of medium. The samples were incubated at 28 °C and 150 rpm for 14 days (Lai et al. 2014). The mycelium was separated from the culture broth and dried at 40 °C.

Finally, the dried mycelium (980 g) was obtained. The mycelia were ultrasonically broken and extracted exhaustively with 85% alcohol (3 × 1 L) at room temperature, filtered under vacuum, and transferred to clean bottles. Ethanol was removed from the solution using a rotary evaporator at 40 °C. The water phase was extracted with ethyl acetate (EtOAc). The organic solvent was evaporated to dryness under reduced pressure, to give 12.8 g of crude extract.

Isolation and purification of compounds

The separated crude EtOAc fraction was first subjected to column chromatography (CC) by eluting the silica gel with a gradient of petroleum ether/EtOAc from 9:1 to 0:10 (v/v). Nine fractions (Fs. A to Fs. I) were obtained based on TLC. Fraction Fs. B (134 mg) dissolved in $CHCl_3$ was chromatographed over a silica gel column with a gradient of petroleum ether/EtOAc from 9:1 to 1:1 (v/v), to afford compound **2** (24 mg). Fraction Fs. C (3.6 g) with CH_3OH was heated to 60 °C and stirred until completely dissolved, and then placed in a ventilation cabinet for evaporation drying. After stewing for 24 h, crystals were formed and washed with methanol three times, to obtain compound **7** (231 mg). The residual liquid was subjected to a Sephadex LH-20 column with an isocratic elution of 1:1 CH_3OH/CH_2Cl_2 (v/v), to obtain compound **3** (165 mg) and Fraction Fs C1. In turn, Fraction Fs C1 was dissolved in acetone and separated by silica gel CC with a gradient of petroleum ether/EtOAc from 9:1 to 1:1 (v/v), to afford compounds **1** (18 mg) and **4** (14 mg). Fraction Fs. D (274 mg) was dissolved in $CHCl_3$ and the solution was separated by silica gel CC using a petroleum ether–EtOAc mixture (20:1 to 1:1), to give compound **5** (16 mg) and subfraction Fs. D1. Fraction Fs. D1 was dissolved in $CH_3OH–CHCl_3$ (1:1) and purified in a Sephadex LH-20 column with an isocratic elution of $CH_3OH–CH_2Cl_2$ (1:1 v/v), to obtain compound **6** (21 mg). The chemical characteristics of the compounds isolated were as follows.

Acetylcholinesterase/butyrylcholinesterase inhibition activity in vitro assay

The determination of the in vitro AChE inhibition activity of the endophytic fungal extracts and compounds **1–7** was conducted according to the method of Ellman's spectrophotometry (Ellman et al. 1961; Devidas et al. 2021). Known AChEIs, i.e., rivastigmine and huperzine A, were used as the positive controls. The assay was carried out in the 96-well microtiter plates. Briefly, a preincubation solution of 250 µL of phosphate buffer (200 mM, pH 7.7) that contained 15 µL of purified compounds/rivastigmine/HupA, 80 µL of DTNB [3.96 mg of DTNB and 1.5 mg of sodium bicarbonate dissolved in 10 mL of phosphate buffer (pH 7.7)], and 10 µL of AChE/BuChE was prepared. The mixture was incubated for 5 min at 25 °C. After preincubation, 15 µL of the substrate AChI/BChI (10.85 mg in 5 mL of phosphate buffer) was added and incubated again for 5 min. The color developed was measured in a microwell plate reader at 412 nm (Bio-Rad, Hercules, CA). Percent inhibition was calculated through the following formula: (control absorbance − sample absorbance)/control absorbance × 100.

Kinetic study of acetylcholinesterase inhibition

According to Ellman's method, a kinetic analysis of AChE was performed (Ellman et al. 1961; Sonmez et al. 2017). The type of inhibition was deduced by determining K_m and V_{max} using Lineweaver–Burk reciprocal plots by plotting $1/V$ against $1/S$ at varying concentrations of the acetylthiocholine substrate (0.01–0.04 mM). The inhibitory constant, K_i, was calculated by secondary plots obtained by plotting $1/V$ versus different inhibitor concentrations.

Docking study

The preparation of ligand file includes three aspects: (i) draw the small molecular structure of ligand by drawing software; (ii) minimize the energies of small ligand molecules drawn; (iii) initialization of small molecule docking of ligand. In the first step, the two-dimensional structural formulae of asteric acid, methyl asterrate, and ethyl asterrate were drawn using ChemBioDraw Ultra 14.0 drawing software, and the files were saved in ".mol" format. In the second step, open the ".mol" file with ChemBio3D Ultra 14.0, minimize the energy using MMFF94 position in the software, and save the minimized molecule as a ".pdb" file for the next step. The third step is to open the ".pdb" format file processed in the previous step with AutoDockTools software, and process the small ligand molecules, including adding Gasteiger charge, detecting the root of ligand, setting the number of rotating structures, etc. All parameters here are default values. The processed ligand molecule is saved as a coordinate file in ".pdbqt" format for molecular docking backup. The ".pdbqt" format file is a file containing atomic coordinates, AutoDock atomic type, charge, and torsion bond information (Pan et al. 2019).

The AutoDock v.4 software was used in the docking simulations. The crystallographic structures of AChE (PDB: 1F8U) (Kryger et al. 2000) and its ligands were processed with AutoDock Tools (version 1.5.6, Sep_17_14) to delete water, add hydrogens, compute Gasteiger charges, and select rotatable side-chain bonds. Affinity (grid) maps of 60 × 100 × 60 points with a grid spacing of 0.375 Å were generated using the help of the program AutoGrid v.4 program included in the AutoDock 4 distribution (Singh et al. 2020; Devidas et al. 2021). AutoDock parameter settings and distance dielectric functions were used in the calculation of

van der Waals and electrostatic terms, respectively (Kumar et al. 2021; Singh et al. 2021). The receptor site is semi-flexible docked with the ligand. The receptor site is maintained as rigid, while the ligand is treated as flexible (Singh et al. 2020). The docking simulation was performed using the "Lamarckian Genetic Algorithm" method and the following associated parameters: 150 individuals in a population with a maximum of 2,500,000 energy evaluations and a maximum of 27,000 generations, the maximum number of top individuals that automatically survive is usually set to 1, the rate of gene mutation in the genetic algorithm is 0–1, and the default value is 0.02, followed by 100 iterations of Solis and Wets local search. Other parameter values were kept in default. The final figures were generated using the Discovery Studio Visualizer program (Accelrys) (Meng et al. 2012a, b; Kou et al. 2021).

Results

Identification of the endophytic fungal FL15

Strain FL15 was cultured in CYA medium at 28 °C for 7 days. The colony diameter can reached 35–40 mm; its color was goose yellow; and the surface mycelium was white and fluffy, slightly convex in the middle, and had yellow droplet of exudation and a flat back (Fig. 2A). In the same culture conditions on PDA, the colony diameter was 46–50 mm; its color was yellow velvet; and the mycelium bulged in the middle, with no droplet exudation on the surface. With the extension of culture time, the color of the front of the colony deepened from yellow to dark yellow, whereas the color of the back and front remained the same (Fig. 2B). In the meanwhile, the strain FL15 was cultured on YES medium at 28 °C for 7 days. The colony diameter was 36–40 mm; its color was white velvet; and it had a flat surface, was slightly bulged in the middle, and a pale-yellow edge at the back, whereas the colony center was white (Fig. 2C). Furthermore, a scanning electron microscopy observation showed that the mycelia of this strain were slender and bamboo-like, with many branches. Clustered conidia were observed in the head, and most broom-like branches were bicycles. There were elliptical or nearly spindle-shaped densely distributed spores near the mycelia, and the walls were smooth (Fig. 2D). The mycelium had a slender septate, was branched, and the wall was smooth (Fig. 2E, F). Based on the colony and cell morphological observation, strain FL15 was recognized as a member of the genus *Talaromyces*. (Fig. 2).

The length of the ITS, 18S rDNA, and 28S rDNA sequence was 589, 1708, and 940 bp, respectively. The accession number(s) for the ITS, 18S rDNA, and 28S rDNA

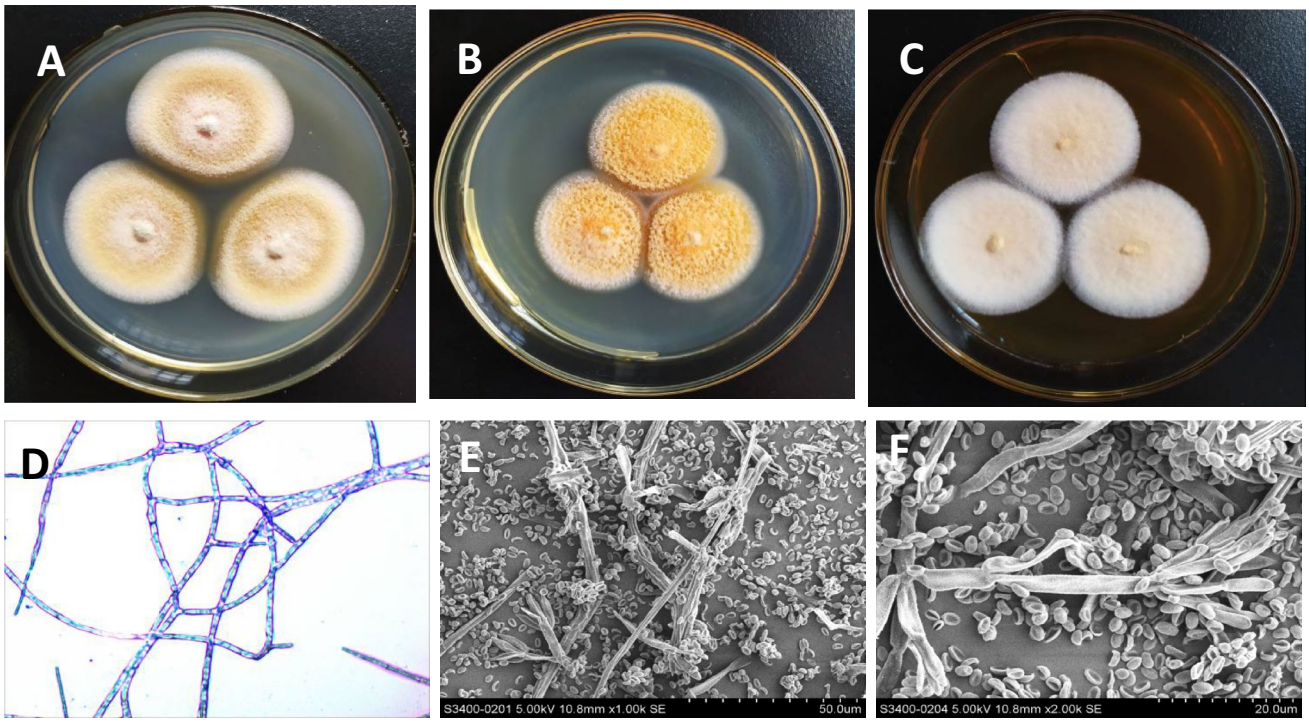

Fig. 2 Colony morphology and mycelium morphology of the endophytic fungus FL15. Colony characteristics of FL15 on CYA (**A**), PDA (**B**); and YES (**C**), respectively; microscopic morphology of FL15 (100×) (**D**); scanning microscopy-based electron micrograph morphology of FL15 (bar = 50 μm) (**E**); scanning electron microscopy-based micrograph morphology of FL15 (bar = 20 μm) (**F**)

nucleotide sequences of the strain FL15 in GenBank were MZ542471, MZ540308, and MZ540309, respectively. BLAST analysis of ITS of strain FL15 showed 99% of sequence similarity with *T. aurantiacus*. Based on the ITS, 18S rDNA, and 28S rDNA sequence analysis, strain FL15 was identified as belonging to the phylum *Ascomycota*, order *Eurotiales,* family *Trichocomaceae*, and genus *Talaromyces*. A phylogenetic tree was constructed using the neighbor-joining and MEGA 7.0.14. By combining the results of morphological observation analysis and those ITS, 18S rDNA, and 28S rDNA sequence phylogenetic analysis, the strain FL15 was identified as *T. aurantiacus* FL15 (Fig. 3).

Structural elucidation of the purified compounds

A total of seven natural compounds were isolated and purified from the crude ethyl acetate extract of the mycelia of the endophytic fungus *T. aurantiacus* FL15. Their chemical structures were elucidated based on ^{1}H nuclear magnetic resonance (NMR), ^{13}C NMR, and electrospray ionization/mass spectrometry (ESI–MS) analyses (Supplementary Tables S1–S3), as well as via the comparison of their properties and spectral characteristics with published data. The compounds were confirmed as being asterric acid **(1)** (Hargreaves et al. 2002), and its derivatives, methyl asterrate **(2)** (Hargreaves et al. 2002), and ethyl asterrate **(3)** (Li et al. 2008), together with four other compounds, emodin **(4)** (Li et al. 2008), physcion **(5)** (Guo et al. 2011), chrysophanol **(6)** (Guo et al. 2011), and sulochrin **(7)** (Liu et al. 2015). The chemical structures of the compounds are depicted in Fig. 4.

Anti-acetylcholinesterase/butyrylcholinesterase activity

The AChE/BuChE inhibitory activities of the purified compounds were evaluated using Ellman's spectrophotometric method, with rivastigmine and Hup A as the reference compounds. The half-maximal inhibitory concentrations (IC_{50}) of the compounds for AChE/BuChE inhibition are summarized in Table 1. The results showed that compounds **1–3** exhibited moderate AChE inhibitory activities, whereas the four other compounds displayed no AChE inhibitory activities. The tested compounds did not afford any inhibition of BuChE. Based on these results, the asterric acid derivatives could be described as being highly selective AChEIs. Moreover, compound **3** exhibited better inhibition against AChE, with an IC_{50} value of 20.1 μM than did compounds **2** (IC_{50} = 23.3 μM) and **1** (IC_{50} = 66.7 μM).

The ability of a compound to cross the blood–brain barrier (BBB) is essential for AD treatment. Thus, log *P* was an important physicochemical parameter for the evaluation or prediction of the ability of the compounds to cross the BBB. The log *P* values of the isolated compounds were calculated

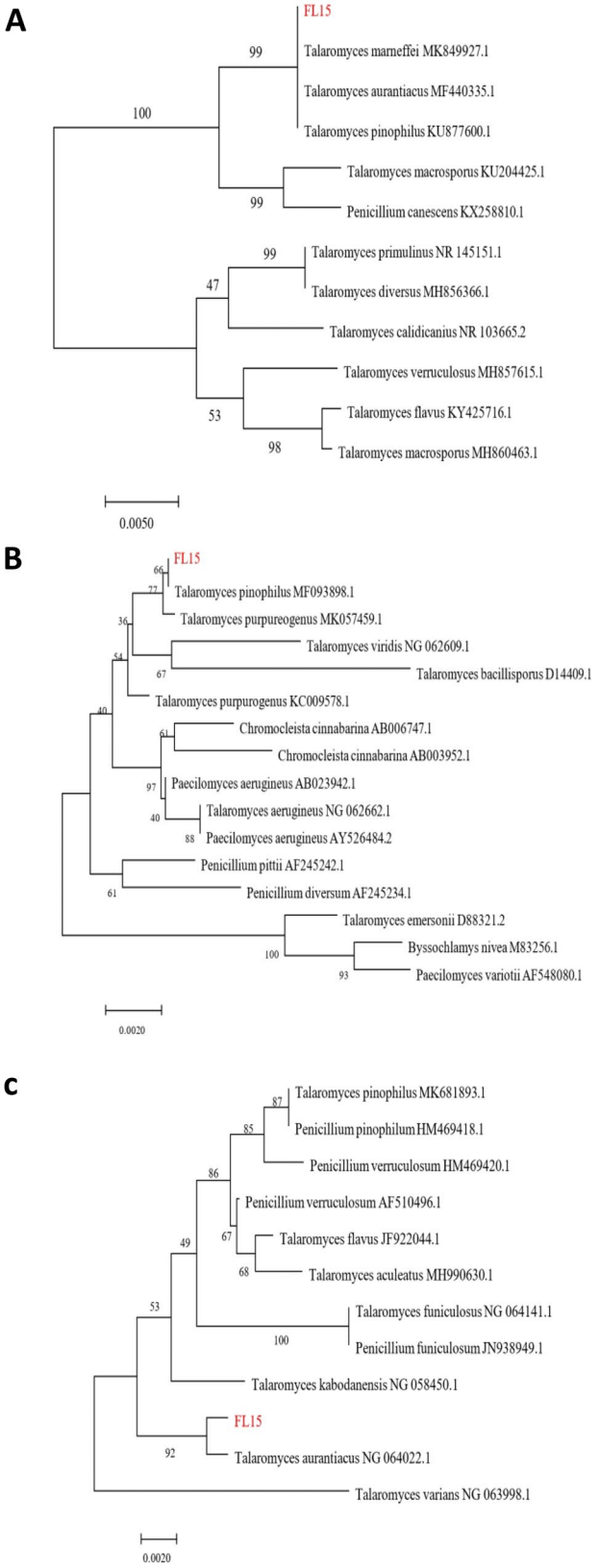

Fig. 3 Phylogenetic tree of strain FL15 and corresponding strains based on ITS (**A**), 18S rRNA (**B**), and 28S rRNA (**C**) sequences

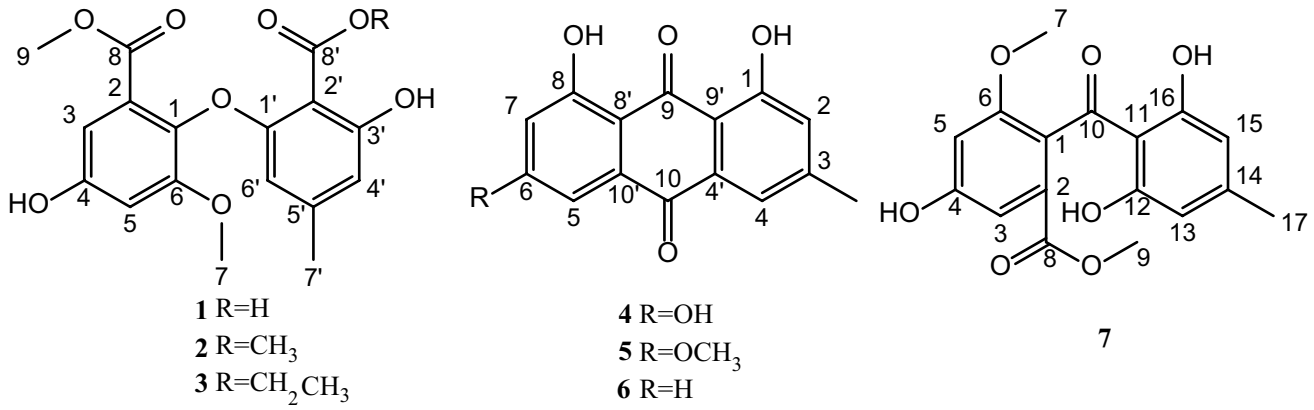

Fig. 4 Structures of compounds 1–7 isolated from FL15

Table 1 Acetylcholinesterase (AChE) and butyrylcholinesterase (BuChE) inhibitory activities and log P values of the title compounds

Compound	IC_{50} ± SEM (μM)[a]		Selectivity index[b]	log *P*
	AChE	BuChE		
1	66.7 ± 1.7	> 100	> 1.50	1.36
2	23.3 ± 1.2	> 100	> 4.29	2.78
3	20.1 ± 0.9	> 100	> 4.98	3.17
4	> 100	> 100	–	
5	> 100	> 100	–	
6	> 100	> 100	–	
7	> 100	> 100	–	
Rivastigmine	1.82 ± 0.13		–	1.34
Huperzine A	0.045 ± 0.01		–	1.22

[a]IC50 values represent the means ± SEM of three parallel measurements ($P < 0.05$)

[b]Selectivity index = IC50 (BuChE)/IC50 (AChE). "–" no determination

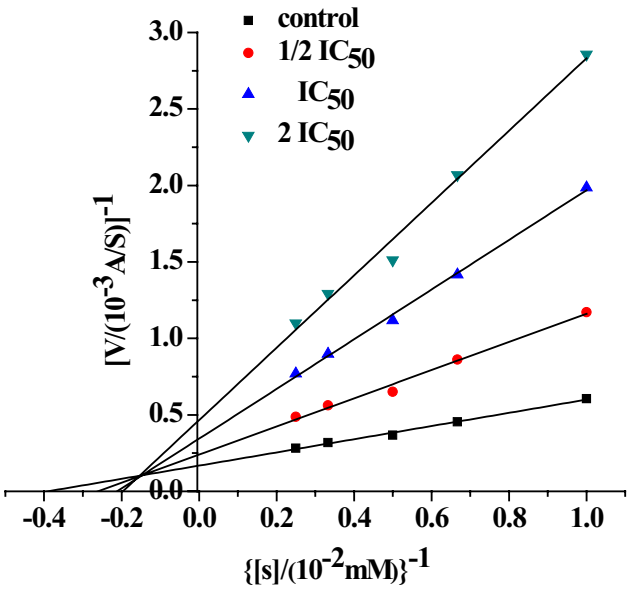

Fig. 5 Kinetic study of the inhibition mode of AChE by compound 3. Overlaid Lineweaver–Burk reciprocal plots of AChE initial velocity at increasing substrate concentration (0.01–0.04 mM) in the absence of inhibitor and the presence of different concentrations of compound 3 are shown

using Lipinski's Rule of Five (http://www.scfbio-iitd.res.in/software/drugdesign/lipinski.jsp) and are shown in Table 1. The optimum log *P* value for central nervous system penetration is around 2 ± 0.7. Thus, the log *P* results indicated that the isolated compounds were sufficiently lipophilic to pass the BBB.

Kinetic study of acetylcholinesterase inhibition

The crystal structure of AChE in complex with inhibitors revealed the presence of dual binding sites: a Ser–His–Glu catalytic site (CAS) located at the bottom of the gorge, and a peripheral anionic-binding site (PAS) located at the gorge entrance (Bartus et al. 1982; Miles and Ross 2021). An enzyme kinetic study was performed to explore the AChE inhibition mode of compounds **1–3**. The results obtained from in the reciprocal Lineweaver–Burk plot (Fig. 5) show increased slopes (decreased V_{max}), and intercepts (higher K_m) at higher inhibitor concentrations, and a mixed-type inhibition was demonstrated. Therefore, compounds **1–3** might be able to simultaneously bind to CAS and PAS, as well as the catalytic triad of AChE. The inhibitory constant, K_i (0.14 mM), was determined by plotting the slopes of the Lineweaver–Burk reciprocal plots versus the concentrations of compound **3**.

Docking study

Docking studies were performed using AutoDock 4 to analyze the binding mode of the asterric acid derivatives to AChE (PDB ID: 1F8U) (Kryger et al. 2000). From the docking results, AChE interacted with compound **1** through 14 amino acid residues, namely, Asp73, Trp85, Gly119, Tyr123, Ser124, Tyr132, Glu201, Ser202, Phe292, Tyr332, Phe333, His471, and Tyr 473. Hydrogen-bond interaction with Asp73, Gly119, Tyr123, Ser124, Tyr132, Glu201, and Ser202, π–π interactions with Trp85, π–σ interactions with Tyr332, π-alkyl interactions with Phe292, Phe333, and Tyr 473, and carbon–hydrogen bonds with His471 was observed (Fig. 6.1A–C). The methyl ester group of benzene ring interacts with His471 by van der Waals force at a distance of about 3.12 Å, and with Ser202 by hydrogen bonding at a distance of about 2.12 Å. Whereas, AChE interacted with compound **2** through 15 amino acid residues, hydrogen bonds with residues Asp73, Gly119, Gly120, Tyr123, Ser124, Tyr132, Glu201, and Ser202, π–σ interactions with Tyr332, π-alkyl interactions with Phe292 and Phe333, and carbon–hydrogen bonds with Thr82, Trp85, Asn86, and His471 (Fig. 6.2A–C). Compared to the interaction between compound **1** and electric eel AChE, the ester bond site of methyl asterrate at the peripheral anion site formed hydrogen bond with Thr82 and Asn86. These two hydrogen bonds were the non-existent interaction between compound **1** and electric eel AChE, which may increase the interaction force between methyl asterrate and the peripheral anion site. Compound **3** interacted AChE through 14 amino

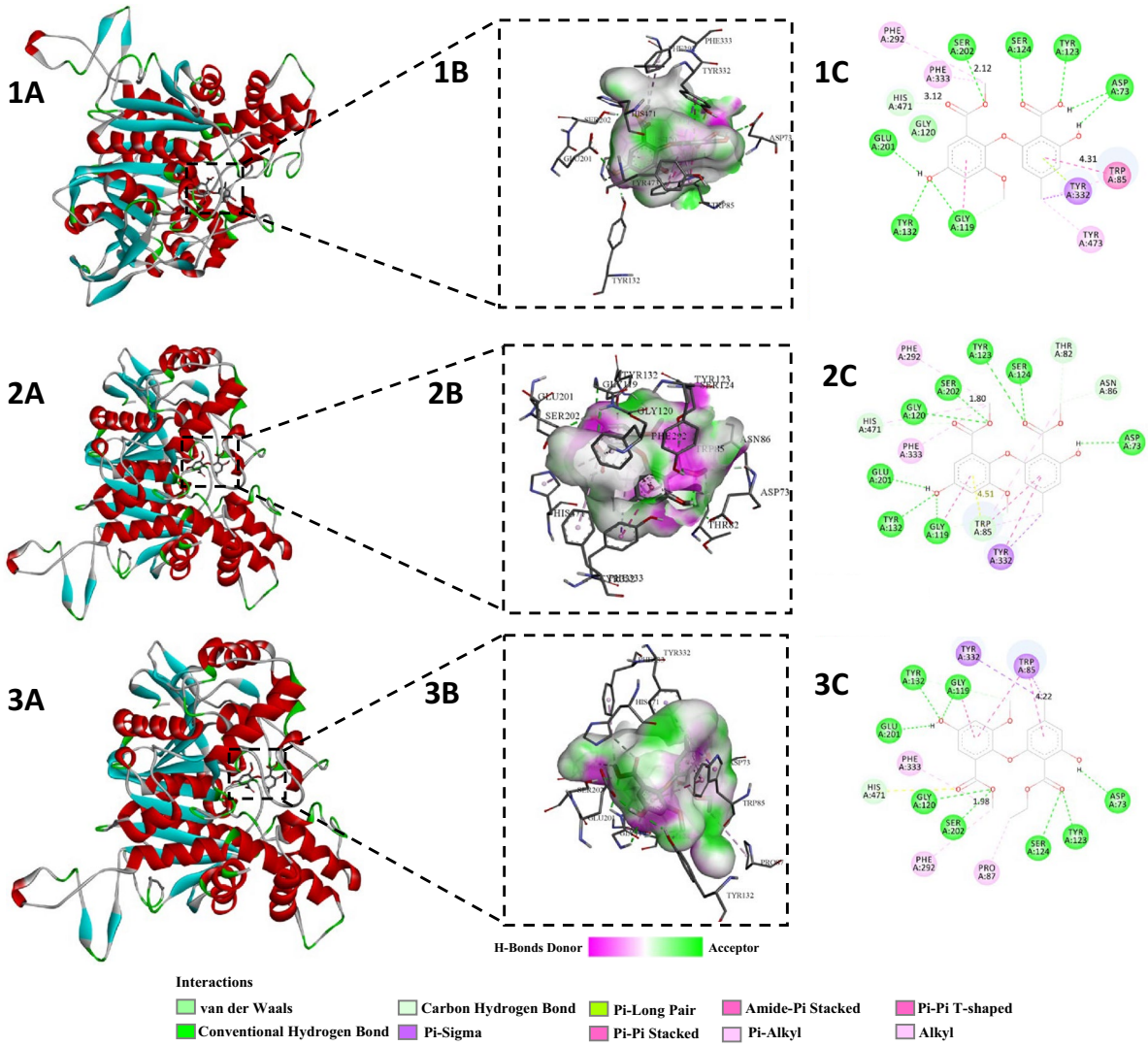

Fig. 6 Diagrams the docking poses (**A**), interactions (**B**), and two-dimensional interactions (**C**) of asterric acid (**1**), methyl asterrate (**2**), and ethyl asterrate (**3**) docked to AChE (PDB: 1F8U). The dashed lines represent bonding interactions. The interacting amino acid residues are labeled. The figures were generated using the Discovery Studio Visualizer software (Accelrys)

acid residues. Compound **3** formed hydrogen bonds with residues Asp73, Gly119, Gly120, Tyr123, Ser124, Tyr132, Glu201, Ser202, π–σ interactions with residues Trp85, Tyr332, π-alkyl interactions Pro87, Phe292, and Phe333, while His471 exhibited carbon–hydrogen-bond interaction (Fig. 6.3A–C). The values of the free energy of binding (ΔG) for the 'asteric acid–AChE', 'methyl asterrate–AChE' and 'ethyl asterrate–AChE' interactions were − 7.89, − 9.72, and − 9.74 kcal/mol, respectively, and their corresponding IC_{50} values were estimated to be 66.7, 23.3, and 20.1 μM, respectively (Kryger et al. 2000; Shaikh et al. 2015). The active site of AChE was reported to be located at the bottom of a deep and narrow gorge, consisting of a number of domains. The peripheral anion site is located at the entrance of the active pocket, which comprises residues Trp85 and Trp304. The catalytic active site for AChE of electric eels composed of Ser202, Glu325, His471, Trp85, and Trp304. From the docking results in Fig. 6, Compound 1–3 could enter the active cavity of electric eelfish AChE and interact with the amino acids of the peripheral anion sites in the active cavity and the main amino acids of the catalytic active center. Ser202 and His471 interact with the catalytic active center mainly by hydrogen bond, and Trp85 and so on form π–π stacking interaction. At the bottom of the gorge, the benzene ring structure of the diphenyl ether interacted with Trp85 via π–π stacking, and the oxygen atom of the ester group created a hydrogen bond with the hydroxyl group of Tyr123 (Xu et al. 2020; Miles and Ross 2021). In summary, the asteric acid derivatives can interact with both peripheral activity sites (PAS) and catalytic activity sites (CAS) of AChE.

Discussion

AChEIs were initially isolated from plants (Su et al. 2017). However, the production of AChEIs through plant extraction processes is limited due to the lack of natural plant resources. Meanwhile, marked-available AChEIs derived from plants showed a lot of disadvantages such as low bioavailability and other abdominal side effects. Thus, exploring other alternatives of AChEIs derived from microbial sources with different niches is a must (Su et al. 2017; Zaki et al. 2020). Endophytes are a rich source of bioactive and chemically novel compounds with huge medicinal and agricultural potential. Furthermore, they can produce bioactive substances identical or similar to those of host plants (Su et al. 2017; Zaki et al. 2020). Hence, searching for a natural, cost-effective, and sustainable source of effective AChEIs from endophytes has become an attractive subject for many researchers (Su et al. 2017; Zaki et al. 2020). So far, various structural types of AChEIs, including alkaloids, terpenoids, and other compounds, were found in fungi, especially endophytic fungi (Table 2), suggesting that fungi represent valuable, novel, and alternative resources with good AChE inhibitory activity (Su et al. 2017; Zaki et al. 2020). To date, more than 300 endophytic fungal isolates from *H. serrata* have been isolated, of which 9 endophytic fungal strains can produce Hup A (Cao et al. 2021). Additionally, avertoxin B isolated from endophytic fungi of *H. serrata* showed AChE inhibitory activity (IC_{50}, 14.9 μM) (Wang et al. 2015). Herein, we also isolated diphenyl ethers AChEIs from endophytic fungi of *H. serrata*.

The existed studies showed that fungal AChEIs displayed different AChE inhibitory activity with IC_{50} from 0.026 μM to 280 μM (Table 2). Our result showed that asteric acid derivatives (compounds **1**–**3**) exhibited AChE inhibitory activities with IC_{50} values of 66.7, 23.3, and 20.1 μM, respectively. Compared to IC_{50} values of other AChEIs derived from fungi, the asteric acid derivatives exhibited moderate AChE inhibitory activity (Table 2). Meanwhile, asteric acid derivatives have no inhibitory activities against BuChE (Table 1), indicating that asteric acid derivatives have high selectivity.

According to the available reports, the asteric acid derivatives were firstly isolated from the fermentation broth of *Aspergillus terreus* in 1960 (Curtis et al. 1960). Thereafter, these metabolites were gradually discovered in fungi that belong to different genera, such as *Penicillium frequentans* (Mahmoodian and Stickings 1964), *Oospora sulfureaochracea* (Natori and Nishikawa 1962), *Scytalidium* spp. (Stermits et al. 1973), *Pestalotiopsis* spp. (Ogawa et al. 1995; Liu et al. 2009), *Phoma* sp. (Jayasuriya et al. 1995), *Geomyces* sp. (Li et al. 2008), and *A. flavipes* (Zhang et al. 2016), as well as in endophytic fungi, such as *Neoplaconema napellum* IFB-E016 from *Hopea hainanensis* (Wang et al. 2006), *Aspergillus* sp. F1 from *Trewia nudiflora* (Lin et al. 2009), and *Pseudogymnoascus* sp. from the Antarctic marine sponge *Hymeniacidon* spp. (Figueroa et al. 2015). To the best of our knowledge, these three asterric acid derivatives were isolated from the genus *Talaromyces* for the first time.

Asteric acid and its analogs have attracted considerable interest as the first non-peptide endothelin-1-binding inhibition (Ohashi et al. 1992). Thus, asteric acid, as a vascular endothelial growth factor inhibitor and antibiotic, has been commercialized as a biological reagent and used in biological and medical-related research (Tang et al. 2007). Furthermore, several asteric acid derivatives are useful for treating myocardial infarction and renal insufficiency (Curtis et al. 1960). Asteric acid and its analogs also exhibit other good or excellent medicinal activities. Dimethyl 2,3-dimethoxyosoate and 2-(2-formyl-3-hydroxy-5-methylphenoxy)-5-hydroxy-3-methoxybenzoate displayed cytotoxicity against the K562 cell line (Liu et al. 2006) and low cytotoxic activity in HepG2 and Raji cells (Fang et al. 2012), respectively. Geomycins B and C displayed substantial antifungal activity

Table 2 Various AChEIs derived from fungi

	Compounds	Strains	Sources	Inhibitory activity against AChE (IC_{50})	References
Alkaloid	Dimeric indole derivatives **1**	*Rubrobacter radiotolerans*	*Petrosia* sp.	11.8 μM	Li et al. (2015)
	Dimeric indole derivatives **2**			13.5 μM	
	Quinolactacins A1	*Penicillium citrinum*	Soil sample	280 μM	Kim et al. (2001)
	Quinolactacins A2			19.8 μM	
	Cytochalasin H	*Phomopsis* sp. Cs-c2	*Senna spectabilis*	25.0 μg	Chapla et al. (2014)
	Penicinoline	*Penicillium steckii* SCSIO 41,025	Mangrove	87.3 μM	Chen et al. (2021)
	Penicinoline E			68.5 μM	
Meroterpene	Arigsugacin I, Arigsugacins F, Territrem B	*Penicillium* sp. sk5GW1L	*Kandelia candel*, China	0.64 ± 0.08 μM	Huang et al. (2013)
	Isoaustinol	*Aspergillus* sp. 16–5	Mangrove	2.50 μM	Long et al. (2017)
	Dehydroaustin			0.40 μM	
	Dehydroaustinol			3.00 μM	
	Arigsugacin	*Penicillium sp.* FO-4259	Soil sample	1 nM	Omura et al. (1995)
Sesquiterpenoid	Colletotrichine B	*Colletotrichum gloeosporioides* GT-7	*Uncaria rhynchophylla*	38.0 ± 2.67 μg/mL	Chen et al. (2019)
	Armiloid A	co-culture of *Armillaria* sp. and endophytic fungus *Epicoccum* sp.	*Gastrodia elata*	4.91 μM	Li et al. (2019)
	Talaromycin A	*Talaromyces marneffei*	Epilobium angustifolium	12.63 μM	Yang et al. (2021)
Diterpene	Trachyloban-17,19-dioic acid	*Syncephalastrum racemosum*	–	0.06 μM	Santos et al. (2018)
Polyketide	Avertoxin B	Endophytic fungus	*Huperzia serrata*	14.9 μM	Wang et al. (2015)
	Koninginin T	*Phomopsis stipata*	*Styrax camporum* Pohl	10.0 μg (galantamine was employed as positive control at 1.0 μg)	Biasetto et al. (2020)
Phenol	14-(2′, 3′, 5′-trihydroxyphenyl) tetradecan-2-ol	*Chrysosporium sp.*	Not clear	197 μM	Sekhar Rao et al.(2001)
Benzopyranones	Palmariol B	*Hyalodendriella sp.* Ponipodef12	*Populus deltoides*	115.31 μg/ml	Meng et al. (2012b)
	4-hydroxymellein			116.05 μg/ml	
	Alternariol 9-methyl ether			135.52 μg/ml	
	Botrallin			103.70 μg/ml	
Oxaphenalenone Xanthenone	Talaromycesone A	*Talaromyces* sp. Strain LF458	*Axinella verrucosa*	7.49 ± 0.08 μM	Wu et al. (2014)
	Talaroxanthenone			1.61 ± 0.26 μM	
	Isopentenylxanthenone			2.60 ± 0.03 μM	
Diketopiperazines	Cyclo-(L-Val-L-Pro)	*Aspergillus sydowii*	Soil and a voucher specimen	0.36 ± 0.17 μmol mL^{-1}	Lima et al. (2018)
Lipopeptide	Sinulariapeptides A	*Cochliobolus Lunatus* SCSIO41401	marine alga *Coelarthrum* sp.	1.8 ± 0.12 μM	Dai et al. (2020)
	Sinulariapeptides B			1.3 ± 0.11 μM	
Glycerol ether	Phthalide glycerol ether			2.5 ± 0.21 μM	
Cyclohexanoids	Speciosin U	*Saccharicola* sp.	*Eugenia jambolana*	0.026 ± 0.005 mg/ml	Chapla et al. (2020)
Carboxylic acid	Trans-3,4-dihydro-3,4-dihydroxy-anofinic acid			0.053 ± 0.007 mg/ml	

Table 2 (continued)

	Compounds	Strains	Sources	Inhibitory activity against AChE (IC_{50})	References
Oxysporone	Pestalrone C	*Pestalotiopsis* sp. YMF1.0474	–	33.90 μM	Liu et al. (2021)
	6-[1-hydroxy-(1S)-pentyl]-4-methoxy-(6S)-2H,5H-pyran-2-one			81.54 μM	
	LL-P880β			16.43 μM	
	Pestalrone A			95.22 μM	

against *A. fumigatus* and antimicrobial activities against Gram-positive and Gram-negative bacteria, respectively (Li et al. 2008). More recently, methyl asterrate, methyldichloroasterrate, methyl 3-chloroasteric acid, monomethylosoic acid, and 2,4-dichloroasteric acid exhibited more potent inhibitory activities against α-glucosidase *vs.* acarbose (Wang et al. 2016a, b; Zhang et al. 2016). Herein, we showed for the first time that asteric acid and its derivatives displayed highly selective AChE inhibitory activities.

To further reveal the relationship between asteric acid derivatives and acetylcholinesterase and the reasons for the differences activities of asteric acid derivatives, the molecular docking analysis was carried out. Docking is a structure-based drug design method, which can effectively estimate the binding energy and conformation of drugs (Devidas et al. 2021). Docking results show that the three asteric acid derivative molecules could interact with PAS and CAS of eel AChE. One of the benzene rings of diphenyl ether binds through hydrogen bonding and π–π interaction with the key amino acid residues of peripheral sites, while another substituent of the benzene ring interacts with center of the catalytic activity. Among them, the hydrophobic ester bond and hydrophobic benzene ring formed a large hydrophobic pocket with hydrophobic amino acid residues such as Gly119, Gly120, Phe292, and Phe333. These interactions enable the three small molecules to bind well to the electric eel AChE, and thus compete with the substrate to inhibit the AChE activity. Pan et al (2019) reported that linarin improves the dyskinesia by inhibiting AChE. To assess whether linarin could dock with AChE and decipher mechanism of linarin as AChEI, molecular docking simulation was used. The result shows that linarin may inhibit AChE by binding to the hydrophobic active site of the alkoxy substrate including residues Phe 330 and Phe 331. This active site is different from our docking result of AChE inhibition by simultaneously binding to CAS and PAS. In comparison with the docking results of Devidas et al. 2021, our result is consistent with those of previous studies in which the same amino acid residues of AChE played an essential role in substrate binding. The IC_{50} values of asteric acid **(1)**, methyl asterrate **(2)**, and ethyl asterrate **(3)** were 66.7, 23.3, and 20.1 μM, respectively, which suggests that the size and variety of the esterification substituent at C-8′ on the parent nucleus may contribute to the AChE inhibitory activities of these compounds. Moreover, a kinetic analysis revealed a mixed-type AChE inhibition of diphenyl ether compounds (Kou et al. 2021). Therefore, the AChE inhibitory activities of diphenyl ether compounds are important to identify their structure–activity relationships and design compounds with higher activity based on this lead compound. Accordingly, the asteric acid scaffold could be considered in the design of a new AChEI.

Conclusions

In the present study, three natural compounds asteric acid (**1**), methyl asterrate (**2**), and ethyl asterrate (**3**) possessed a diphenyl ether structure were isolated from endophytic fungal *T. aurantiacus* FL15 of *H. serrata*. These compounds exhibited potent AChE inhibitory activities, with IC_{50} values of 66.7, 23.3, and 20.1 μM, respectively. Docking analysis results not only showed that they displayed selectivity inhibitory activities to AChE, and their action against AChE was related to esterification R groups of 8 carbon on the parent nucleus, but also demonstrated binding interactions with the PAS and CAS of the enzyme. According to the calculated log P values, all three compounds might pass the BBB. To the best of our knowledge, this study was the first to report on asteric acid derivatives that act as AChEIs. Asteric acid could be considered as a new lead scaffold to develop more potent AChEIs.

Supplementary Information The online version contains supplementary material available at https://doi.org/10.1007/s13205-022-03125-2.

Acknowledgements This study was supported by Natural Science Foundation of China (81760649), the Natural Science Foundation of Jiangxi Province of China (20181BAB215044), and Funds of Jiangxi Science and Technology Normal University (2017XJZD004).

Author contributions YWX designed and performed all experiments under the supervision of DZ, and developed the manuscript draft. WZL and DL supervised studies on the experiments on identification of endophytic fungi, isolation and purification of compound. ZBZ and JC analyzed the experimental data and discussed the results with the coauthors and revised this manuscript.

Declarations

Conflict of interest The authors have no conflict of interest to declare.

References

Bartus RT, Dean RL, Beer B et al (1982) The cholinergic hypothesis of geriatric memory dysfunction. Science 217:408–417. https://doi.org/10.1126/science.7046051

Biasetto CR, Somensi A, Sordi R et al (2020) The new koninginins T-U from *Phomopsis stipata*, an endophytic fungus isolated from *Styrax camporum* pohl. Phytochem Lett 36:106–110

Cao D, Sun P, Bhowmick S et al (2021) Secondary metabolites of endophytic fungi isolated from *Huperzia serrata*. Fitoterapia 155:104970. https://doi.org/10.1016/j.fitote.2021.104970

Chapla VM, Zeraik ML, Ximenes VF et al (2014) Bioactive secondary metabolites from *Phomopsis* sp., an endophytic fungus from *Senna spectabilis*. Molecules 19:6597–6608. https://doi.org/10.3390/molecules19056597

Chapla VM, Honório AE, Gubiani JR et al (2020) Acetylcholinesterase inhibition and antifungal activity of cyclohexanoids from the endophytic fungus *Saccharicola* sp. Phytochem Lett 39:116–123

Chen XW, Yang ZD, Li XF et al (2019) Colletotrichine B, a new sesquiterpenoid from Colletotrichum gloeosporioides GT-7, a fungal endophyte of *Uncaria rhynchophylla*. Nat Prod Res 33:108–112. https://doi.org/10.1080/14786419.2018.1437437

Chen CM, Chen WH, Pang XY et al (2021) Pyrrolyl 4-quinolone alkaloids from the mangrove endophytic fungus *Penicillium steckii* SCSIO 41025: Chiral resolution, configurational assignment, and enzyme inhibitory activities. Phytochem 186:112730

Curtis RF, Hassall CH, Jones DW et al (1960) The biosynthesis of phenols. Part II. Asterric acid, a metatoblic product of *Aspergillus terreus* Thom. J Chem Soc. https://doi.org/10.1039/JR9600004838

Dai Y, Li K, She J et al (2020) Lipopeptide epimers and a phthalide glycerol ether with AChE inhibitory activities from the marine-derived fungus *Cochliobolus Lunatus* SCSIO41401. Mar Drugs 18:547. https://doi.org/10.3390/md18110547

Devidas SB, Rahmatkar SN, Singh R et al (2021) Amelioration of cognitive deficit in zebrafish by an undescribed anthraquinone from *Juglans regia* L: an in-silico, in-vitro and in-vivo approach. Eur J Pharmacol 906:174234. https://doi.org/10.1016/j.ejphar.2021.174234

Ellman GL, Courtney KD, Andres V et al (1961) A new and rapid colorimetric determination of acetylcholinesterase activity. Biochem Pharmacol 7:88–95. https://doi.org/10.1016/0006-2952(61)90145-9

Fang MJ, Fang H, Li WJ et al (2012) A new diphenyl ether from *Phoma* sp. strain, SHZK-2. Nat Prod Res 26:1224–1228. https://doi.org/10.1080/14786419.2011.559947

Figueroa L, Jimenez C, Rodríguez J, et al (2015) 3-Nitroasterric acid derivatives from an antarctic sponge-derived *Pseudogymnoascus* sp. fungus. J Nat Prod 78:919–923. https://doi.org/10.1021/np500906k

Friker LL, Scheiblich H, Hochheiser IV et al (2020) β-Amyloid clustering around ASC fibrils boosts its toxicity in microglia. Cell Rep 30:3743-3754.e6. https://doi.org/10.1016/j.celrep.2020.02.025

Goedert M, Spillantini MG (2006) A century of Alzheimer's disease. Science 314: 777–781. https://science.sciencemag.org/content/314/5800/777

Guo S, Feng B, Zhu R et al (2011) Preparative isolation of three anthraquinones from *Rumex japonicus* by high-speed counter-current chromatography. Molecules 16:1201–1210. https://doi.org/10.3390/molecules16021201

Gupta S, Chaturvedi P, Kulkarni MG et al (2019) A critical review on exploiting the pharmaceutical potential of plant endophytic fungi. Biotechnol Adv 39:107462. https://doi.org/10.1016/j.biotechadv.2019.107462

Hargreaves J, Park JO, Ghisalberti EL et al (2002) New chlorinated diphenyl ethers from an *Aspergillus* species. J Nat Prod 65:7–10. https://doi.org/10.1021/np0102758

Huang X, Sun X, Ding B et al (2013) A new anti-acetylcholinesterase α -pyrone meroterpene, arigsugacin I, from mangrove endophytic fungus *Penicillium* sp. sk5GW1L of *Kandelia candel*. Planta Med 79:1572–1575

Jalili-Baleh L, Babaei E, Abdpour S et al (2018) A review on flavonoid-based scaffolds as multi-target-directed ligands (MTDLs) for Alzheimer's disease. Eur J Med Chem 152:570–589. https://doi.org/10.1016/j.ejmech.2018.05.004

Jayasuriya H, Ball RG, Zink DL et al (1995) Barceloneic acid A, a new farnesyl-protein transferase inhibitor from a *Phoma* species. J Nat Prod 58:986–991. https://doi.org/10.1021/np50121a002

Kim W, Song N, Yoo CD (2001) Quinolactacins Al and A2, new acetylcholinesterase inhibitors from *Penicillium citrinum* in MeOH was further purified by reverse phase HPLC. J Antibiot (tokyo) 54:831–835

Kingston DG (2011) Modern natural products drug discovery and its relevance to biodiversity conservation. J Nat Prod 74:496–511. https://doi.org/10.1021/np100550t

Kou X, Liu J, Chen Y et al (2021) Emodin derivatives with multi-factor anti-AD activities: AChE inhibitor, anti-oxidant and metal chelator. J Mol Struct 1239:130459. https://doi.org/10.1016/j.molstruc.2021.130459

Kryger G, Harel M, Giles K et al (2000) Structures of recombinant native and E202Q mutant human acetylcholinesterase complexed with the snake-venom toxin fasciculin-II. Acta Crystallogr D Biol Crystallogr 56:1385–1394. https://doi.org/10.1107/S0907444900010659

Kumar S, Bhardwaj VK, Singh R et al (2021) Explicit-solvent molecular dynamics simulations revealed conformational regain and aggregation inhibition of I113T SOD1 by Himalayan bioactive molecules. J Mol Liq 339:116798. https://doi.org/10.1016/j.molliq.2021.116798

Lai Z, Wang D, Wang Y et al (2014) Molecular identification of endophytic fungi with inhibitory activityagainst acetylcholinesterase from *Huperzia serrata*. Mycosystema 33: 858–866. http://journals.im.ac.cn/jwxten/ch/reader/view_abstract.aspx?file_no=jw14040858&flag=1

Li Y, Sun B, Liu S et al (2008) Bioactive asterric acid derivatives from the antarctic ascomycete fungus *Geomyces* sp. J Nat Prod 71:1643–1646. https://doi.org/10.1021/np8003003

Li JL, Huang L, Liu J et al (2015) Acetylcholinesterase inhibitory dimeric indole derivatives from the marine actinomycetes *Rubrobacter radiotolerans*. Fitoterapia 102:203–207. https://doi.org/10.1016/j.fitote.2015.01.014

Li HT, Tang L, Liu T et al (2019) Polyoxygenated meroterpenoids and a bioactive illudalane derivative from a co-culture of *Armillaria* sp. and *Epicoccum* sp. Org Chem Front 6:3847–3853. https://doi.org/10.1039/C9QO01087D

Lima GS, Rocha AM, Santos GF et al (2018) Metabolic response of *Aspergillus sydowii* to OSMAC modulation produces acetylcholinesterase inhibitors. Phytochem Lett 24:39–45. https://doi.org/10.1016/j.phytol.2018.01.007

Lin T, Lu CH, Shen YM (2009) Secondary metabolites of *Aspergillus* sp. F1, a commensal fungal strain of *Trewia nudiflora*. Nat Prod Res 23:77–85. https://doi.org/10.1080/14786410701852826

Liu R, Zhu W, Zhang Y et al (2006) A new diphenyl ether from marine-derived fungus *Aspergillus* sp. B-F-2. J Antibiot 59:362–365. https://doi.org/10.1038/ja.2006.52

Liu L, Li Y, Liu S et al (2009) Chloropestolide A, an antitumor metabolite with an unprecedented spiroketal skeleton from *Pestalotiopsis fici*. Org Lett 11:2836–2839. https://doi.org/10.1021/ol901039m

Liu D, Yan L, Ma L et al (2015) Diphenyl derivatives from coastal saline soil fungus *Aspergillus iizukae*. Arch Pharm Res 38:1038–1043. https://doi.org/10.1007/s12272-014-0371-z

Liu WC, Gong T, Zhu P (2016) Advances in exploring alternative taxol sources. RSC Adv 6:48800–48809. https://doi.org/10.1039/C6RA06640B

Liu CM, Wang YL, Wang X et al (2021) Active metabolites from the fungus *Pestalotiopsis* sp. ymf1.0474. Chem Nat Comp 57:1–3

Long Y, Cui H, Liu X et al (2017) Acetylcholinesterase inhibitory meroterpenoid from a mangrove endophytic fungus *Aspergillus* sp. 16–5c. Molecules 22:727. https://doi.org/10.3390/molecules22050727

Ma X, Tan C, Zhu D et al (2007) Hup A from *Huperzia* species—an ethnopharmacological review. J Ethnopharmacol 113:15–34. https://doi.org/10.1016/j.jep.2007.05.030

Mahmoodian A, Stickings CE (1964) Studies in the biochemistry of micro-organisms. 115. Metabolites of *Penicillium frequentans* westling: isolated of sulochrin, asterric acid, (+)- bisdechlorogeodin and two new substituted anthraquinones, questin and questinol. Biochem J 92:369–378. https://doi.org/10.1042/bj0920369

Meng FC, Mao F, Shan WJ et al (2012a) Design, synthesis, and evaluation of indanone derivatives as acetylcholinesterase inhibitors and metal-chelating agents. Bioorg Med Chem Lett 22:4462–4466. https://doi.org/10.1016/j.bmcl.2012.04.029

Meng X, Mao Z, Lou J et al (2012b) Benzopyranones from the endophytic fungus *Hyalodendriella* sp. Ponipodef12 and their bioactivities. Molecules 17:11303–11314. https://doi.org/10.3390/molecules171011303

Miles JA, Ross BP (2021) Recent advances in virtual screening for cholinesterase inhibitors. ACS Chem Neurosci 12:30–41. https://doi.org/10.1021/acschemneuro.0c00627

Mohammadi-Khanaposhtani M, Saeedi M, Zafarghandi NS et al (2015) Potential acetylcholinesterase inhibitors: design, synthesis, biological evaluation, and docking study of acridone linked to 1, 2, 3-triazol derivatives. Eur J Med Chem 92:799–806. https://doi.org/10.1016/j.ejmech.2015.01.044

Natori S, Nishikawa H (1962) Structures of osoic acids and related compounds, metabolites of *Oospora sulphurea-ochracea* v. BEYMA Chem Pharm Bull 10:117–124. https://doi.org/10.1248/cpb.10.117

Ogawa T, Ando K, Aotani Y et al (1995) RES-1214-1 and 2, novel non-peptidic endothelin type a receptor antagonists produced by *Pestalotiopsis* sp. J Antibiot (tokyo) 48:1401–1406. https://doi.org/10.1002/chin.199623286

Oh JM, Kang MG, Hong A et al (2019) Potent and selective inhibition of human monoamine oxidase-B by 4-dimethylaminochalcone and selected chalcone derivatives. Int J Biol Macromol 137:426–432. https://doi.org/10.1016/j.ijbiomac.2019.06.167

Ohashi H, Akiyama H, Nishikori K et al (1992) Asterric acid, a new endothelin binding inhibitor. J Antibiot 45:1684–1685. https://doi.org/10.7164/antibiotics.45.1684

Omura S, Kuno F, Otoguro K et al (1995) Arisugacin, a novel and selective inhibitor of acetylcholinesterase from *Penicillium* sp. FO-4259. J Antibiot 4:745–746

Pan H, Zhang J, Wang Y et al (2019) Linarin improves the dyskinesia recovery in Alzheimer's disease zebrafish by inhibiting the acetylcholinesterase activity. Life Sci 222:112–116. https://doi.org/10.1016/j.lfs.2019.02.046

Prince PM, Wimo A, Guerchet M et al (2015) The global impact of dementia: word Alzheimer report 2015. Washington: ADI. https://www.alzint.org/resource/world-alzheimer-report-2015/

Santos GF, Lima GS, Oliveira GP et al (2018) New AChE inhibitors from microbial transformation of trachyloban-19-oic acid by *Syncephalastrum racemosum*. Bioorg Chem 79:60–63. https://doi.org/10.1016/j.bioorg.2018.04.011

Sekhar Rao KC, Divakar S, Karanth NG et al (2001) (2', 3', 5' -Trihydroxyphenyl) tetradecan-2-ol, a novel acetylcholinesterase inhibitor from *Chrysosporium* sp. J Antibiot (tokyo) 54:848–849

Shaikh S, Zainab T, Shakil S et al (2015) A neuroinformatics study to compare inhibition efficiency of three natural ligands (Fawcettimine, Cernuine and Lycodine) against human brain acetylcholinesterase. Netw-Comp Neur 26:25–34. https://doi.org/10.3109/0954898X.2014.994145

Singh R, Bhardwaj VK, Sharma J et al (2020) Discovery and in silico evaluation of aminoarylbenzosuberene molecules as novel checkpoint kinase 1 inhibitor determinants. Genomics 113:707–715. https://doi.org/10.1016/j.ygeno.2020.10.001

Singh R, Bhardwaj VK, Sharma J et al (2021) Identification of selective cyclin-dependent kinase 2 inhibitor from the library of pyrrolone-fused benzosuberene compounds: an in silico exploration. J Biomol Struct Dyn 5:1–9. https://doi.org/10.1080/07391102.2021.1900918

Sonmez F, Zengin Kurt B, Gazioglu I et al (2017) Design, synthesis and docking study of novel coumarin ligands as potential selective acetylcholinesterase inhibitors. J Enzyme Inhib Med Chem 32:285–297. https://doi.org/10.1080/14756366.2016.1250753

Stermits FR, Schroeder HA, Geigert J (1973) Asterric acid from *Scytalidium*. Phytochemistry 12:1173. https://doi.org/10.1016/0031-9422(73)85038-1

Su J, Liu H, Guo K et al (2017) Research advances and detection methodologies for microbe-derived acetylcholinesterase inhibitors: a systemic review. Molecules 22:176. https://doi.org/10.3390/molecules22010176

Tang H, Zhen Y, Lao X et al (2007) Research progress in receptor antagonists from microorganisms. World Notes Antibiot 28:19–24. http://en.cnki.com.cn/Article_en/CJFDTOTAL-GYKS200701004.htm

Teles APC, Takahashi JA (2013) Paecilomide, a new acetylcholinesterase inhibitor from *Paecilomyces lilacinus*. Microbiol Res 168:204–210. https://doi.org/10.1016/j.micres.2012.11.007

Vig R, Bhadra F, Gupta SK et al (2021) Neuroprotective effects of quercetin produced by an endophytic fungus *Nigrospora oryzae* isolated from *Tinospora cordifolia*. J Appl Microbiol. https://doi.org/10.1111/jam.15174

Wang FW, Ye YH, Chen JR et al (2006) Neoplaether, a new cytotoxic and antifungal endophyte metabolite from *Neoplaconema napellum* IFB-E016. FEMS Microbiol Lett 261:218–223. https://doi.org/10.1111/j.1574-6968.2006.00358.x

Wang M, Sun M, Hao H et al (2015) Avertoxins A-D, prenyl asteltoxin derivatives from *Aspergillus versicolor* Y10, an endophytic fungus of *Huperzia serrata*. J Nat Prod. https://doi.org/10.1021/acs.jnatprod.5b00600

Wang C, Guo L, Hao J et al (2016a) α-glucosidase inhibitors from the marine-derived fungus *Aspergillus flavipes* HN4-13. J Nat Prod 79:2977–2981. https://doi.org/10.1021/acs.jnatprod.6b00766

Wang Y, Lai Z, Li XX et al (2016b) Isolation, diversity and acetylcholinesterase inhibitory activity of the culturable endophytic fungi harboured in *Huperzia serrata* from Jinggang Mountain, China. World J Microbiol Biotechnol 32:20. https://doi.org/10.1007/s11274-015-1966-3

Wu B, Ohlendorf B, Oesker V et al (2014) Acetylcholinesterase inhibitors from a marine fungus *Talaromyces* sp. strain

LF458. Mar Biotechnol 17:110–119. https://doi.org/10.1007/s10126-014-9599-3

Xu K, Zhou Q, Li XQ et al (2020) Cadinane- and drimane-type sesquiterpenoids produced by *Paecilomyces* sp. TE-540, an endophyte from *Nicotiana tabacum* L., are acetylcholinesterase inhibitors. Bioorg Chem 104:104252. https://doi.org/10.1016/j.bioorg.2020.104252

Yang ZD, Zhang XD, Yang X et al (2021) A norbisabolane and an arabitol benzoate from *Talaromyces marneffei*, an endophytic fungus of *Epilobium angustifolium*. Fitoterapia 153:104948

Zaki AG, El-Sayed ER, Abd Elkodous M et al (2020) Microbial acetylcholinesterase inhibitors for Alzheimer's therapy: recent trends on extraction, detection, irradiation-assisted production improvement and nano-structured drug delivery. Appl Microbiol Biotechnol 104:4717–4735. https://doi.org/10.1007/s00253-020-10560-9

Zhang D, Yang Y, Castlebury LA et al (1996) A method for the large scale isolation of high transformation effificiency fungal genomic DNA. FEMS Microbiol Lett 145:261–265. https://doi.org/10.1016/S0378-1097(96)00421-1

Zhang ZB, Zeng QG, Yan RM et al (2011) Endophytic fungus *Cladosporium cladosporioides* LF70 from *Huperzia serrata* produces Huperzine A. World J Microbiol Biotechnol 27:479–486. https://doi.org/10.1007/s11274-010-0476-6

Zhang LH, Feng BM, Zhao YQ et al (2016) Polyketide butenolide, diphenyl ether, and benzophenone derivatives from the fungus *Aspergillus flavipes* PJ03-11. Bioorg Med Chem Lett 26:346–350. https://doi.org/10.1016/j.bmcl.2015.12.009